CRESSON, R., DABERT, P., BERNET, N. - 2009. Microbiology and performance of a methanogenic biofilm reactor during the start-up period. Journal of Applied Microbiology, vol. 106, n° 3, p. 863 - 876

author-produced version of the final draft post-refeering
The original publication is available at http://www.blackwell-synergy.com - doi:10.1111/j.1365-2672.2008.04055.x

Microbiology and performance of a methanogenic biofilm reactor during the start-up period

Romain Cresson[1,2], Patrick Dabert[1,3], Nicolas Bernet[1]

1 INRA, UR50, Laboratoire de Biotechnologie de l'Environnement, Avenue des Etangs, Narbonne, F-11100, France.

2 ITE, 1, avenue du Forum, 11781 Narbonne Cedex.

3 CEMAGREF, UR GERE, 17, avenue de Cucillé CS 64427 35044 Rennes cedex, France (present adress).

Abbreviated running headline: Start-up of a methanogenic biofilm reactor

Correspondence : Nicolas Bernet, INRA, UR50,Laboratoire de Biotechnologie de l'Environnement, Avenue des Etangs, Narbonne, F-11100, France.

E-mail : bernet@supagro.inra.fr

Aims: to understand the interactions between anaerobic biofilm development and process performances during the start-up period of methanogenic biofilm reactor.

Methods and results: Two methanogenic Inverse Turbulent Bed Reactors (ITBR) have been started and monitored for 81 days. Biofilm development (adhesion, growth, population dynamic) and characteristics (biodiversity, structure) were investigated by using molecular tool (PCR-SSCP, FISH-CSLM). Identification of the dominant populations, in relation to process performances and to the present knowledge of their metabolic activities, was used to propose a global scheme of the degradation routes involved. The inoculum which determines the microbial species present in the biofilm influences bioreactor performances during the start-up period. FISH observations revealed a homogeneous distribution of the Archaea and bacterial populations inside the biofilm.

Conclusion: This work points out the link between biodiversity, functional stability and methanogenic process performances during start-up of anaerobic biofilm reactor. It shows that inoculum and substrate composition greatly influence biodiversity, physiology and structure of the biofilm.

Significance and Impact of the Study : The combination of molecular techniques associated to a biochemical engineering approach is useful to get relevant information on the microbiology of a methanogenic growing biofilm, in relation with the start-up of the process.

Keywords: Biofilm, Anaerobic digestion, Bioreactor start-up, Microbial population dynamics, Methanogenesis, Acetogenesis.

Introduction

Anaerobic digestion is an effective method for treating many organic wastes. Compared with aerobic process, the advantages are : lower energy requirement, higher treatment efficiency, lower sludge amount and valuable gas production (Lettinga *et al.* 1983). The limitation of anaerobic digestion processes resides in the duration and instability of their transitory phases (starting, restarting, organic load increase) because of the anaerobic microorganisms low growth rate and sensitivity to perturbations such as organic overloads (Henze *et al.* 1983; Weiland *et al.* 1991; Austermann-Haun *et al.* 1994; Puñal *et al.* 2001; Arnaiz *et al.* 2003).

The natural ability of microorganisms to aggregate between them and/or to adhere on a solid surface and form a biofilm can be exploited to improve significantly the efficiency of anaerobic wastewater treatment processes by increasing their capacity of microbial biomass retention (Hall 1987; Annachhatre 1996). If the advantages of fixed biomass processes for anaerobic digestion have been underlined (*i.e.* biomass retention, robustness, high loads…) (Nicolella *et al.* 2000), the optimization of the start-up period seems necessary to increase the competitiveness of anaerobic high rate processes. This initial phase can be defined as the time required for the selection and organisation of an effective microbial consortium for a given pollutant (Weiland *et al.* 1991; Heppner *et al.* 1992). Regarding process performances, the objective of this phase is to reach as quickly as possible the process nominal load with the desired treatment efficiency without creating instability of the anaerobic ecosystem.

For Heijnen *et al.* (1989) however, the organic load increase during start up should not be related to a criterion of treatment performance, but rather with criteria of biological activities. During start-up, a continuous and progressive load increase should occur while preserving an optimal biological activity in order to respect as well as possible biomass nutritional requirements to avoid transitory shocks (Stronach *et al.* 1986). Hence, the influent organic composition would significantly select the microorganisms involved in the anaerobic biofilm

formation and more precisely the proportions of hydrogenotrophic and acetoclastic methanogens (Ehlinger *et al.* 1989). However, until recently, it was difficult to assess the microbiology of such processes, which is now more accessible thanks to the development of molecular tools. Thus, FISH and/or molecular fingerprints (DGGE, SSCP) have been recently used to study the dynamic transition of a methanogenic population in a thermophilic digester (Hori *et al.*, 2006), the microbial community and population dynamics in an anaerobic hybrid reactor (Boonapatcharoen *et al.*, 2007), or the microbial community during biofilm development in an Upflow Anaerobic Sludge Bed (UASB) reactor (Fernandez *et al*, 2008).

It is clear that controlling the anaerobic processes start-up requires a thorough knowledge of the biological processes and microorganisms which implement them. The objective of the present study was to establish a link between process performances and implementation, evaluated during the start-up period of two anaerobic three phase reactors and the microbiology of their corresponding ecosystems. The installation of biofilm microbial communities was investigated by 16S rRNA targeted PCR and Single Strand Conformation Polymorphism (SSCP) capillary electrophoresis of the PCR products (Zumstein *et al.* 2000). Moreover, colonized particles were observed at the end of the start-up period by FISH using a confocal laser scanning microscopy to get information on the spatial distribution of the Archae and bacterial communities in the biofilm.

Materials and methods

Experimental set-up

The reactors used for this study were two inverse turbulent bed biofilm reactors. With this process, anaerobic biomass is grown on low density particles that are fluidised by an up-flow current of biogas recirculated from the top of the reactors. Because of an important solubilisation of CO2 in the liquid phase, the biogas was mainly composed of methane

(>90%). Biogas injection velocity is used to control the height of fluidization and clogging problems. The reactors had an active volume of 7.24 L and were filled with the solid carrier material up to 24% of its active volume. This coke manufacture residue (U-Spheres™, provided by Omega Minerals, Hamburg – Deutschland) is a mineral granular material composed mainly of silica and alumina. The solid particles had an average equivalent diameter of 172 µm and a specific density of 696 $g.L^{-1}$. The use of such a small particulate carrier increases considerably the area available for biofilm growth. Further details on experimental devices, carrier characteristics and operational parameters are available in a previous study (Cresson *et al.* 2006).

Operating conditions

Both reactors were inoculated with 3 litres of a sludge at 13.6 $g.L^{-1}$ of volatile suspended solids (VSS) gathered from a pilot scale fixed bed anaerobic digester ($1m^3$) treating winery wastewater. Sludge specific activity was measured at 3 successive times in batch mode, in a 6 litres reactor, with ethanol as the only substrate. It was equal to 0.11 $g_{COD}.g_{VSS}^{-1}.d^{-1}$ for the third essay (COD, chemical oxygen demand).

The influent used in this work was a wine-based wastewaterconsisting of diluted red wine (ethanol as the carbon substrate) complemented with nitrogen as NH_4Cl and phosphorus as NaH_2PO_4, at a ratio of COD/N/P equal to 400/7/1 and, from day 58 until the end of the experiment, with a solution of trace elements at concentration of 5 ppm. The dilution factor was adapted to the potential of the microbial consortium. The COD concentration of the influent was increased from 0.5 to 20 g_{COD}.L-1 from the beginning to the end of the start-up period. Influent was stored at 4°C. Composition of the influent and trace element combination are reported in a previous study (Cresson *et al.* 2006).

During the inoculation period, both reactors have been operated in batch mode for 12 hours in order to enhance attachment of planktonic bacteria on the solid carrier (Cresson *et al.*

2007). In the meantime, the sludge was recycled from the bottom to the top of the reactor with a peristaltic pump, to ensure a good contact between the microorganisms and the carrier. After this short inoculation period, a continuous inlet flow of diluted wastewater was applied to maintain a constant hydraulic retention time of 24 hours, in order to enhance biofilm formation and to minimize planktonic bacterial growth in the liquid phase by encouraging their washout (Tijhuis *et al.* 1994; Michaud *et al.* 2005; Cresson *et al.* 2008). Thereafter, the only difference between both reactors was the start-up strategy applied to increase the organic loading rate (OLR) and to bring both reactors to their expected organic load and removal efficiency.

For strategy A (reactor R_A), the wine concentration in the influent was stepwise increased (from 0.25% to 10%) when the reactor COD removal efficiency reached 80%. The hydraulic retention time (HRT) was kept constant and equal to one day. For the maximum load strategy (reactor R_B), the reactor was frequently submitted to pulse injections of wastewater. The effect of these disturbances on the amount of biogas produced by the digester was analysed. In case of a decreased biogas production (e.g. the disturbance induces an overload of the reactor), the loading rate was decreased (or kept constant) (Steyer *et al.* 1999). In case of an increased biogas production, the loading rate was increased by increasing the wine concentration in the influent as above. In both strategies, the objective was to increase the COD load of the reactor from 0.5 to 20 $g_{COD}.L^{-1}.d^{-1}$ as quickly as possible without inhibiting the system.

Reactor monitoring

pH, biogas and liquid flow rates, biogas composition, total suspended solids (TSS), volatile suspended solids (VSS), attached volatile solids (AVS), volatile fatty acids (VFA), bicarbonate (HCO_3^-), and chemical oxygen demand (COD) were routinely analyzed according to the methods described in (Cresson *et al.* 2006).

Samples preservation and total genomic DNA extraction

Two millilitres of colonized particles were sampled from the reactors using a disposable syringe and gently washed 3 times with 10 millilitres of PBS 1X buffer. These washed colonized particles were ground in 500 µl of Guanidine Thiocyanate 4M-Tris-Cl 0.1M pH 7.5 and 150 µl of N-Lauroyl sarcosine 10% using a mortar. 500 µl samples were immediately frozen and stored at –20 °C. Total genomic DNA was extracted from frozen pellets using the QIAAMP DNA STOOL kit (QIAGEN, France) according to supplier instruction. DNA purity, integrity and concentration were assessed by 0.7% agarose gel electrophoresis and ethidium bromide staining.

Bacterial and archaeal 16S rDNA-targeted PCR-SSCP amplifications

For bacterial community, the PCR – SSCP was performed by direct amplification of the 16S rRNA gene (16S rDNA) V3 region using the W49-W104 primer couple. Primers sequences were: W49 AGGTCCAGACTCCTACGGG (forward, *E. coli* position 330 (Brosius *et al.* 1981)) and W104 TTACCGCGGCTGCTGGCAC (reverse, *E. coli* position 533). Primer W104 was labelled with the 5'-FAM fluorochrome (Applied Biosystems, Perkin-Elmer). PCR reaction mix was as follow: about 100 ng of total DNA, *Pfu* turbo supplied buffer 1X, dNTP 0.2 mM each, primers 2.6 ng/µl each, H_2O up to 50 µl and 1.25 U of *Pfu* turbo DNA polymerase (Stratagene). After an initial denaturation step of 2 min at 94°C, 25 cycles were applied with 30 s at 94°C, 30 s at 61°C and 30 s at 72°C. Reactions were ended by a 10 min elongation at 72°C and cooling at 4°C.

For archaeal community, the PCR – SSCP attempted by direct amplification of the 16S rRNA gene did not give a positive signal on faintly colonised particles, probably because of the low amount of biomass attached to the particles. A nested PCR protocol was thus applied as follow. A first amplification of the total archaeal 16S rDNA was performed using primers W17 ATTCYGGTTGATTCCYGSCRG (forward, *E. coli* position 6); W02

GNTACCTTGTTACGAAACTT (reverse, *E. coli* position 1492) and the Red *Taq* DNA polymerase (Sigma). Reaction mix was the same as above except for the Red *Taq* DNA polymerase enzyme and buffer. PCR reaction was started by a denaturation step of 2 min. at 94°C followed by 30 cycles of 1 min at 94°C, 1 min at 50°C and 1 min at 72°C. Reaction was ended by a 10 min elongation at 72°C and cooling at 4°C. PCR products were then diluted 100 times and used for a V3 region-targeted PCR – SSCP using primers W104 and W116 TCCAGGCCCTACGGGG (forward *Archaea*, E. coli position 333). Reaction mix and PCR conditions using *Pfu* turbo DNA polymerase (Stratagene) were the same as described above for the bacterial PCR – SSCP reaction, except for primer annealing temperature that was 51°C. All PCR reactions were performed using a GeneAmp PCR system 9700 thermocycler (Applied Biosystems). PCR products size and concentration were estimated by 2% agarose gel electrophoresis and ethidium bromide staining.

SSCP electrophoresis and microbial community profiles analysis

SSCP capillary electrophoresis was performed as described in Delbès *et al.* (2000). One µl of PCR – SSCP product (diluted 10 to 20 times in water) was mixed with 18.8 µl of formamide and 0.2 µl of the internal standard GS-400 Rox (Applied Biosystems). The samples were then denaturated 5 min at 95°C and placed directly on ice for 5 min. The resulting single-stranded DNA fragments were separated by capillary electrophoresis using a CAP 5.58 %-Glycerol 10% polymer and the ABI 310 Genetic Analyser equipped with a capillary tube (47 cm x 50 mm) (Applied Biosystems). Laser detection of the sample PCR products and internal standards generated molecular typing profiles (so called SSCP profiles) that were aligned and compared using the GeneMapper software (Applied Biosystems). To facilitate comparison when a large number of profiles was analysed, each profile was scanned and represented as a row of discs where each disc corresponds to a distinguishable peak with its area being proportional to the peak proportion in the total profile.

Identification of the dominant peaks revealed on SSCP profiles was obtained as described in Dabert *et al*. (2001). Briefly, the 16S rDNA V3 region of bacterial and archaeal

communities were amplified again from total genomic DNA as described above but using the Red*Taq* DNA polymerase (Sigma) and unlabeled primers. The resulting PCR products were purified with the QIAquick Spin kit (Quiagen) before to be cloned into *E. coli* using the TOPO TA cloning kit according to supplier instructions (Invitrogen). *E. coli* with inserts of proper size (about 200 bp) were screened by PCR on colony using plasmid-targeted primers (T7 and M13) and 2% agarose gel electrophoresis. Correct amplified fragments were amplified again using the above PCR-SSCP protocols. All inserts producing a peak that co-migrated with distinguishable peaks from the bacterial or archaeal SSCP profiles were sequenced to finalize the process of peak identification.

DNA sequences were performed by MillGen (Toulouse, France). Sequences were identified by comparison with their closest relative available in databases using Blast from the National Center for Biotechnology Information and the Ribosomal Database Project. DNA sequences have been deposited in the EMBL database under accession numbers AM939911 to AM939923.

Colonized particles FISH

Sample fixation and FISH hybridization were performed using standard conditions (Amann *et al.* 1990) except for colonized particles handling. Colonized particle samples (2 ml) were retrieved from each reactor using a plastic disposable syringe. Sample fixation was performed by sucking three volumes of a 4% paraformaldehyde PBS 1X solution in the syringes, rolling them gently and placing them at 4°C during 3 to 5 hours. The colonized particles were then rinsed 3 times within the syringe by gently sucking in and out PBS 1X buffer. Finally, colonized particles were stored at -20°C in a 1:1 PBS 1X and absolute ethanol solution. For hybridization, fixed particles were rinsed once with hybridization buffer and then hybridization was carried out in 0.6 mL Eppendorf tubes by soaking the colonized particles in 500 µL of 20% formamide hybridization solution (Amann et al., 1990). Labelled

probes (EUB338 - CY3, or ARC915 – FAM, (Batstone *et al.* 2004)) were added to a final concentration of 4ng.L^{-1}. Hybridization was done under gentle agitation at 46°C for 3 hours in the dark. After hybridization, particles were washed twice at 48°C in 2 mL washing solution preheated and under gentle agitation (once for 15 minutes and then for 30 minutes). Total cells labelling was carried out by addition of the DNA specific dye chromomycine to washing solutions. Observations were carried out using a laser scanning confocal microscope Leica TCS SP2 equipped with three lasers (wavelengths of excitation of 633, 543, 488 nm). Microscopic fields were digitized to one µm depth using 40X and 20 X objectives.

Results

Reactors performances

The start-up period of both reactors was investigated for 81 days. A carbon mass balance was drawn up, considering that ethanol was the only organic carbon source in the diluted wine influent and that carbon flux distributed primarily between anabolic reactions (*i.e.* biomass production), and catabolic reactions (*i.e.* biogas and VFA production). These hypotheses were verified by comparing theoretical COD values calculated from ethanol concentration in the influent to COD values measured at different influent organic loads. The differences observed were always below 2% (data not shown). Fig. 1 and Table 1A and 1B summarise reactors performances. The global behaviour of both reactors is similar for the period of time considered. Four phases can be distinguished:

For the first 10 days of experiment (phase I), an OLR of 0.5 $g_{COD}.L^{-1}.d^{-1}$ was applied to both reactors. During this first phase, the part of carbon input converted to methane, after a lag phase of one week, increased quickly and stabilized around 40%. An average of 6 to 8 % of the input carbon was converted into acetate, propionate and butyrate (Table 1), whose

concentration remained below 0.1 $g_{COD}.L^{-1}$. As a consequence COD removal rates increased quickly to reach more than 90% of removal efficiency for both systems (Fig. 1).

Considering the next 28 days (phase II), the OLR was increased from 0.5 $g_{COD}.L^{-1}.d^{-1}$ to 6.5 $g_{COD}.L^{-1}.d^{-1}$ according to each strategy. COD removal rate remained similar for both reactors, above 87% with an average around 92%. The fraction of input carbon metabolized into VFA increased from 6.5% to values as high as 32% on day 30 for the R_A and 17% on day 38 for the R_B. Carbon fractions dedicated to methane production, which were around 40% at the beginning of phase II, dropped accordingly.

From day 38 to 58 (phase III), COD removal efficiency and methane production collapsed for both systems, while VFA accumulated to about 2.5 $g_{COD}.L^{-1}$. The R_A was more affected, with COD removal efficiency falling below 60%. According to strategy A, the OLR was kept stable at 6.5 $g_{COD}.L^{-1}.d^{-1}$. The OLR of R_B was still slightly increased from 6.5 to 10.7 $g_{COD}.L^{-1}.d^{-1}$, while its COD removal efficiency stood above 70%. Chromatographic analysis showed that propionic acid represented 13.5 and 13.4% of total VFA accumulated for R_A and R_B respectively. This VFA accumulation (intermediates and also inhibitors of anaerobic digestion) indicated an incomplete degradation of the substrate and signed more particularly a failure of methanogenesis, the last phase of anaerobic digestion. This failure was due to a lack of micronutrients, in particular cobalt (Co) and nickel (Ni), which were found in very low concentrations in the diluted red wine used as influent (Cresson *et al.* 2006).

Therefore, from day 58 until the end of experiment (phase IV), a solution of trace elements was added to the influent (5 ppm). After 5 days of complementation, high COD removal efficiencies were restored (more than 90 %) in both reactors, VFA concentrations dropped below 0.2 $g_{COD}.L^{-1}$ and the part of input carbon converted into methane exceeded 53% (Fig. 1 and Table 1). OLRs were increased according to their respective strategies until they reached 20.7 for R_A and 23.2 $g_{COD}.L^{-1}.d^{-1}$ for R_B. Considering overall performances

during the 81 days of experiment, the reactor started with strategy B removed 30% more COD, produced 32% more methane and accumulated 19% less VFA than R_A.

Microbial communities dynamics

The microbial community dynamics of both reactors was followed by PCR amplification of microbial 16S rRNA gene V3 variable regions and SSCP capillary electrophoresis of the resulting PCR products (Zumstein et al. 2000). The microbial community profiles obtained were aligned and compared throughout the experiment to reveal population changes within the community. A total of 42 SSCP profiles were analysed: the inoculum sludge and 10 biofilm samples from each reactor (corresponding to days 1, 16, 23, 26, 30, 35, 44, 54, 65 and 72 of experiment) in order to monitor bacterial and archaeal microbial communities dynamics.

Bacterial community dynamics

The first sampling and analysis of carrier particles was done 24 hours after the inoculation period. Comparison of the inoculum and carrier particles SSCP profiles shows a rapid and preferential attachment of a few microbial populations onto the carrier (Fig. 2). Such early microbial attachment had also been observed in a previous study (Cresson *et al.* 2007). While the inoculum produced a complex SSCP profile characteristic of very diverse microbial communities (Loisel *et al.* 2006), both reactor carriers presented simplified and almost identical profiles with only two strongly dominant peaks (E and K in Fig. 2). These peaks co-migrated with distinguishable but not very dominant peaks from the inoculum profile. After 22 more days, carrier particles colonization was underway as it is shown by the appearance of other dominant peaks in the profiles and the increased area under the peaks.

The evolutions of bacterial populations during both reactors start-up are shown in Fig. 3. Broadly, the dominant species changed much between the first 16th days of operation, and remained relatively stable thereafter until the end of the experiment. The dominance of peaks

E and K was progressively replaced by the one of peaks F and J for R_A and peaks G, H and J for R_B.

Identification of the observed SSCP peaks was obtained by constructing two bacterial 16S rDNA V3 region clone libraries from reactor samples retrieved on day 16 for R_A and on day 23 for R_B. These representative samples have been selected according to the presence and the height of their peaks. Screening of 50 bacterial clones was enough to assign all clearly distinguishable peaks of both bacterial profiles (Fig. 3, peaks A to M). At least two independent clones were sequenced for each assigned peak. The resulting sequences, of about 200 bp length, allowed peaks identification at the genus level (table 2). Six out of the 11 peaks identified were related with more than 97% similarity to species or environmental clones belonging to the *Delta proteobacteria* group, as *Geobacter*, *Pelobacter* and the sulfate-reducing *Desulfovibrio* genus. Four belonged to the *Firmicutes*, three of them to the acetogen group *Sporomusa*. The last one belonged to the *Chloroflexi*. Peaks L and M were not identified.

Archaeal community dynamics

The 16S rDNA-targeted SSCP profile obtained from the inoculum archaeal community showed a low diversity with only 7 distinguishable peaks. Evolution of this community in both reactors is shown in Fig. 4. Biofilms from both reactors on day 1 showed almost identical SSCP profiles containing five to six peaks that all co-migrated with peaks present in the inoculum (Fig. 4). Then, on the contrary of bacterial diversity, archaeal diversity remained low during all the experiment with one largely dominant peak. Library construction for peaks identification was done on an archaeal DNA sample obtained from R_A on day 54. PCR–SSCP analyses were conducted on 20 archaeal clones for peaks assignation. All clones co-migrated either with the dominant peak O or with the transient peak N. The former was identified as an

acetotrophic methanogen *Methanosaeta* while the latter was identified as a hydrogenotrophic methanogen *Methanobacterium.*

FISH and CLSM observation

Colonized particles, sampled on day 72, were hybridized with a combination of probes allowing the selective detection of archaeal (probe ARC915 - FAM) and bacterial populations (probe EUB338 - CY3) and observed by confocal scanning laser microscopy (Fig. 5). The pictures showed a relatively homogeneous distribution of archaeal and bacterial populations with a few archaeal clusters disseminated in the totality of the biofilm without preferential localization.

Discussion

In this study, the start up period of two identical anaerobic fluidized bed reactors operated with different strategies has been monitored. The simplified composition of the influent used resulted in the installation of simplified methanogenic ecosystems. Identification of the dominant microbial populations, linked to the present knowledge of their major metabolic activities, can be used to propose a global scheme of the degradation routes involved within each reactor (Fig. 6).

Ethanol degradation

After one day of operation, the dominant microbial populations detected on carrier particles belonged to the *Sporomusa* and the *Desulfovibrio* groups for the bacterial domain and the *Methanosaeta* and *Methanobacterium* groups for the *Archaea*.

The *Sporomusa* are acetogenic bacteria able to grow with many substrates such as pyruvate, lactate, glycerol, methanol, ethanol, formate and fructose. In most cases, and particularly when the electrons donor is ethanol, the final reduced compound is acetate (Kuhner *et al.* 1997; Biebl *et al.* 2000). Alternatively, they can grow as autotrophic

homoacetogens using H_2-CO_2 to produce acetate (Kuhner *et al.* 1997). It can thus be supposed that they took an active part in acetate production in both reactors, thus supporting growth of acetotrophic methanogens like *Methanosaeta*.

The *Desulfovibrio* are type I sulphate-reducing bacteria that use sulphate as terminal electrons acceptor. Many species have the capacity to function either like hydrogen consumers or producers. In a sulphate rich environment, they use simple substrates such as ethanol, fumarate, malate or pyruvate as carbon and energy sources and oxidize it incompletely to form acetate and carbon dioxide by producing hydrogen sulphide (H_2S). They consume hydrogen and compete with the hydrogenotrophic methanogenic *Archaea* (Widdel 1988). On the opposite, in anaerobic environments deprived of sulphate, or in the presence of very weak sulphate concentrations, they can produce hydrogen by using substrates like lactate or ethanol and be involved in an interspecific H_2 transfer with hydrogenotrophic methanogens, represented here by *Methanobacterium*. A study of Raskin et al. (1996) mentions the persistence of a significant number of *Desulfovibrio* in the biofilm of an anaerobic digester in the absence of sulphate.

The sulphate concentration in both processes, or rather the COD/sulphate ratio, will thus strongly influence the metabolism of the *Desulfovibrio* (Percheron *et al.* 1997). In this study, sulphate concentration in the influent increased during all the start-up proportionally to the OLR increase. It varies from 0.75 at the beginning of the experiment for an OLR equal to 0.5 $gCOD.L^{-1}.d^{-1}$ to 30 $mg.L^{-1}$ for an OLR of 20 $gCOD.L^{-1}.d^{-1}$ at the end of the experiment. However, concentrations ratio remained constant (equal to 660) during all the study. This high value of COD/sulphate ratio suggests that the *Desulfovibrio* identified in both reactors had a metabolism turned towards hydrogen production and did not compete with the methanogenic *Archaea* (Hao *et al.* 1996).

Thus, the simplest scenario during the first days after inoculation would be that ethanol was degraded into methane via the two conventional acetotrophic and hydrogenotrophic ways promoted respectively by the *Sporomusa-Methanosaeta* and *Desulfovibrio-Methanobacterium* couples. The absence of visible methane production during the first 10 days of reactors start up and the requirement for a nested PCR for detection of the archaeal groups suggest a very low amount and activity of the methanogenic groups.

After two weeks of run, the two dominant bacterial groups were gradually replaced by other species that differed between reactors A and B. Within R_A, the *Desulfovibrio* population was replaced by a *Pelobacter* population while the initial species of *Sporomusa* was exchanged with another species of the same genus. Members of the *Pelobacter* genus are described either as syntrophic bacteria oxidizing ethanol, propanol and butanol in their corresponding acids thanks to a fermentative metabolism with hydrogen production, or as bacteria consuming hydrogen and ethanol to produce acetate or propionate with simultaneous Fe (III) or sulphate reduction (Laanbroek *et al.* 1982; Schink *et al.* 1987; Tholozan *et al.* 1990). In the presence of sulphate, *Pelobacter propionicus* oxidizes ethanol in acetate by using sulphate as final electrons acceptor. In the absence of sulphate and with high enough hydrogen partial pressure, ethanol is condensed with bicarbonate or acetate to form propionate or butyrate respectively. At low hydrogen partial pressure, the reaction also produces acetate and propionate (Bornstein *et al.* 1948; Braun *et al.* 1981; Eichler *et al.* 1984; Wu *et al.* 1996). Thus, whatever the sulphate and/or hydrogen concentrations were in the reactor, this bacterial group was probably involved in AGV production and acetotrophic methanogenesis.

In R_A, from day 16 to 72, the bacterial community was thus dominated by *Pelobacter* and *Sporomusa* populations whose fermentative metabolisms were turned towards acetate, propionate or butyrate production. This strong acidogenic activity, associated with the decrease of *Archaea* methanogens acetoclastic activity consecutive to micronutrient

limitation, probably took part in the strong accumulation of acetate in R_A during all the initial phase of the study (until the 59th day). Furthermore, acetate accumulation could also be a consequence of the much lower maximum rate of acetate consumption compared to the one of ethanol consumption during syntrophic ethanol degradation by anaerobic biofilm (Wu *et al.* 1991).

Concerning R_B, the *Desulfovibrio* population dominant at the beginning of the experiment was replaced by two *Geobacter* populations while the initial species of *Sporomusa* was exchanged with the same *Sporomusa* species as the one observed in R_A evolution. Within the *Deltaproteobacteria*, members of the genera *Pelobacter*, *Geobacter*, *Desulfuromonas* and *Desulfuromusa* form a monophyletic group (Lovley *et al.* 1995; Lonergan *et al.* 1996). However, in contrast to *Pelobacter*, *Geobacter* species have a respiratory metabolism with Fe (III) or sulphur S_0 serving as common terminal electrons acceptors. They can completely degrade ethanol, acetate and other short-chain fatty acids like butyrate or propionate to carbon dioxide (Cord-Ruwisch *et al.* 1998; Coates *et al.* 2001). The enrichment in *Geobacter* in R_B and the presence of Fe (0.26mg.L^{-1} in the diluted wine before addition of the complementation solution (Cresson *et al.* 2006)) in the reactor feeding (may have brought an alternative metabolic pathway to the acetoclastic activity of the *Sporomusa-Methanosaeta* couple in this reactor.

If the hypothesis presented above can explain the evolution of the dominant microbial populations and process parameters of both reactors, the initial event that conducted to the installation of different microbial communities in the reactors remained unreachable. It certainly appended very early in the process since the *Pelobacter* and *Geobacter* populations that enriched during the reactor start up were already detectable on the particles at day 1.

Reactors stability

The data presented suggest a slightly better performances for the R_B since it removed 30% more COD, produced 32% more methane and accumulated 19% less VFA than R_A during the whole course of the experiment. This advantage could be linked to the slight difference in dominant bacterial populations present in both reactors. During the period of trace element limitation (from days 30 to 54), a slight reduction of the *Pelobacter* dominance compared to the one of *Sporomusa* was observed in R_A, while the same phenomenon was unseen for the *Geobacter/Sporomusa* couple within R_B. While methanogenesis was primarily supported in R_A by acetate production from *Sporomusa* and *Pelobacter* populations, the presence of two *Geobacter* populations in R_B may have bring alternative degradation pathways and provided an advantage to the microbial consortium in term of catabolic opportunities. The largest biodiversity observed in R_B may have also helped the community to support the period of trace element limitation, resulting in a positive impact on the performances and stability of the reactor.

The link between ecosystem biodiversity and process stability have been proposed in other studies (Fernandez et al. (1999; Zumstein *et al.* 2000). These authors have shown independently that the apparent functional stability of two anaerobic digesters was hiding a permanent evolution of their microbial populations (as detected by 16S rDNA-targeted ARDRA or SSCP). In another study, the comparison of two ecosystems subjected to substrate loading shocks, as it was the case in this study for R_B, suggested that the microbial community appearing the most stable in its structure was associated with the greatest functional instability (Fernandez *et al.* 1999). Finally, the advantage of microbial diversity was also pointed out by Schmidt and Ahring (1999): a UASB anaerobic digester inoculated with two species of acetate-consuming methanogenic *Archaea* was more stable and resistant to fluctuations than a second one inoculated with only one species. Our study, like all the

others listed above, provides microbial ecologists with data that point out the link between microbial diversity and functional stability.

Spatial biofilm organization

FISH hybridizations performed on colonized particles at the end of the experiment showed a relatively homogeneous distribution of the archaeal and bacterial populations in the biofilm. As suggested by Batstone et al. (2004), the nature of the substrate probably has a dominating impact on the spatial arrangement of anaerobic digester process biofilms. Complex substrates composed of organic macromolecules (such as brewery or sugarcane refinery effluents) and requiring an important and limiting phase of hydrolysis tends to generate layered distribution of the various trophic groups within the biofilm. Schematically, these biofilms are composed of an external fine layer of acidogenic bacteria and of an internal layer composed of obligate syntrophic bacteria and *Archaea* methanogens. The core of the biofilm is, most of the time, only slightly or even not hybridized indicating an absence of active cells.

Ethanol, the main organic substrate in this study, is small, easily biodegradabile, compact and hydrophilic molecule. These properties favour its diffusion within the biofilm. Furthermore, considering the recent particles colonization, mass transfer phenomena were undoubtedly facilitated by the biofilm low thickness. The bacteria involved in ethanol degradation are not limited by the access to the substrate as it is shown by the strong signal observed in FISH hybridization. Viable and active bacteria cells were hybridized in the whole biofilm, even in zones close to the carrier. The space arrangement of the archaeal and bacterial populations within the biofilm thus seems dictated by the nature of the substrate.

Conclusion

The work presented here aims to contribute to the comprehension of the mechanisms of installation and maturation of anaerobic biofilms, in order to better understand their formation

and improve the start-up phase of bioreactors. This project, which implies a multi-disciplinary approach, consisted into a global apprehension of two systems started with the same initial conditions (same process, same biomass inoculated) but operated under different start-up strategies. Evolution of the reactor performance as well as the microbial biodiversity appeared to be very similar for both systems. Simplification of the bacterial and archaeal ecosystems compared to the inoculum diversity has been observed and could be ascribed to the nature of the feeding influent. Hence, bacterial biodiversity shows an alternation of the dominant populations supposed to ensure similar or identical metabolic functions for anaerobic ethanol degradation. The slight differences between both systems in term of treatment performance could be explained by the dominance of one *Pelobacter* in R_A versus two *Geobacter* populations in R_B. These two *Geobacter* populations may have brought alternative degradation pathways or better adaptive response to trace element limitation and provided an advantage to the microbial consortium of the R_B in term of catabolic opportunities. Hence, the largest biodiversity observed in the R_B seems to have a positive impact on the performances and the stability of the reactor. Furthermore the spatial arrangement of the archaeal and bacterial populations within the biofilm observed by CLSM seems also dictated by the nature of the substrate.

References

Amann, R.I., Krumholz, L. and Stahl, D.A. (1990) Fluorescent-oligonucleotide probing of whole cells for determinative, phylogenetic, and environmental studies in microbiology. *J Bacteriol* **172**, 762–770.

Annachhatre, A.P. (1996) Anaerobic treatment of industrial wastewaters. *Resour Conserv Recy* **16**, 161-166.

Arnaiz, C., Buffiere, P., Elmaleh, S., Lebrato, J. and Moletta R. (2003) Anaerobic digestion of dairy wastewater by inverse fluidization, The inverse fluidized bed and the inverse turbulent bed reactors. *Environ Technol* **24**, 1431-1443.

Austermann-Haun, U., Seyfried, C.F., Zellner, G. and Diekmann, H. (1994) Start-up of anaerobic fixed film reactors, Technical aspects. *Water Sci Technol* **29**(10-11), 297-308.

Batstone, D.J., Keller J. and Blackall L.L. (2004) The influence of substrate kinetics on the microbial community structure in granular anaerobic biomass. *Water Res* **38**, 1390-1404.

Biebl, H., Schwab-Hanisch, H., Sproer, C. and Lunsdorf, H. (2000) *Propionispora vibrioides*, nov gen., nov sp., a new gram-negative, spore-forming anaerobe that ferments sugar alcohols. *Arch Microbiol* **174**, 239-247.

Boonapatcharoen, N., Meepian, K., Chaiprasert, P. and Techkarnjanaruk, S. (2007) Molecular monitoring of microbial population dynamics during operational periods of anaerobic hybrid reactor treating cassava starch wastewater. *Microb Ecol* **54**, 21-30.

Bornstein, B. and Barker, H. (1948) The energy metabolism of *Clostridium kluyveri* and the synthesis of fatty acids. *J Biol Chem* **172**, 659-669.

Braun, M., Mayer, F., Gottschalk, G. (1981) *Clostridium aceticum (Wieringa)*, a microorganism producing acetic acid from molecular hydrogen and carbon dioxide. *Arch Microbiol Mol Biol Rev* **128**, 288-293.

Brosius, J., Dull, T.J. , Sleeter, D.D. and Noller, H.F. (1981) Gene organization and primary structure of a ribosomal RNA operon from *Escherichia coli*. *J Mol Biol* **148**, 107-127.

Coates, J.D., Bhupathiraju, V.K. , Achenbach, L.A. , McInerney, M.J. and Lovley, D.R. (2001) *Geobacter hydrogenophilus*, *Geobacter chapellei* and *Geobacter grbiciae*, three new, strictly anaerobic, dissimilatory Fe(III)-reducers. *Int J Syst Evol Microbiol* **51**, 581-588.

Cord-Ruwisch, R., Lovley, D.R. and Schink, B. (1998) Growth of *Geobacter sulfurreducens* with acetate in syntrophic cooperation with hydrogen-oxidizing anaerobic partners. *Appl Environ Microbiol* **64**, 2232-2236.

Cresson, R., Carrère, H., Delgenès J.P. and Bernet N. (2006) Biofilm formation during the start-up period of an anaerobic biofilm reactor-Impact of nutrient complementation. *Biochem Eng J* **30**, 55-62.

Cresson, R., P. Dabert, J. P. Delgenès and N. Bernet (2007). Inoculation of anaerobic biofilm reactors, use of molecular tools to study early biofilm formation. In *CD Proceedings of the 11th World Congress on Anaerobic Digestion (AD11)*, Brisbane, Australia.

Cresson, R., Escudié, R., Steyer, J.P., Delgenès, J.P., Bernet, N. (2008) Competition between planktonic and fixed microorganisms during the start-up of methanogenic biofilm reactors. *Water Res* **42**, 792-800.

Dabert, P., Sialve, B. , Delgenès, J.P., Moletta, R. and Godon, J.J. (2001) Characterisation of the microbial 16S rDNA diversity of an aerobic phosphorus-removal ecosystem and monitoring of its transition to nitrate respiration. *Appl Microbiol Biotechnol* **55**, 500-509.

Delbès, C., Moletta R. and Godon, J.J. (2000) Monitoring of activity dynamics of an anaerobic digestor bacterial community using 16S rRNA PCR-Single-Strand Conformation Polymorphism (SSCP). *Environ Microbiol* **2**, 506-515.

Ehlinger, F., Audic, J.M. and Faup G.M. (1989) Influence of seeding conditions on initial biofilm development during the start-up of anaerobic fluidized bed reactors. *Water Sci Technol* **21**(4-5), 157-165.

Eichler, B. and Schink, B. (1984) Oxidation of primary aliphatic alcohols by *Acetobacterium carbinolicum* sp. nov., a homoacetogenic anaerobe. *Arch Microbiol* **140**, 147-152.

Fernandez, A., Huang, S., Seston, S., Xing, J., Hickey, R., Criddle, C. and Tiedje, J. (1999) How stable is stable? Function versus community composition. *Appl Environ Microbiol* **65**, 3697-704.

Fernandez, N., Diaz, E. E., Amils, R. and Sanz, J. L. (2008) Analysis of microbial community during biofilm development in an anaerobic wastewater treatment reactor. *Microb Ecol* **56**, 121-132.

Hall, E.R. (1987). Biofilm reactors in anaerobic wastewater treatment. *Biotechnol Adv* **5**, 257-269.

Hao, O.I., Chen, J.M., Huang, L. and Buglass, R.L. (1996) Sulfate-reducing bacteria. *Crit Rev Env Sci Tec* **26**, 155 -187.

Heijnen, J.J., Mulder, A., Enger, W. and Hoeks, F. (1989) Review on the application of anaerobic fluidized bed reactors in wastewater treatment. *Chem Eng J* **41**, B37-B50.

Henze, M. and Harremoes, P. (1983) Anaerobic treatment of wastewater in fixed film reactors - a literature review. *Water Sci Technol* **15**(Copenhagen), 1-101.

Heppner, B., Zellner, G. and Diekmann, H. (1992) Start-up and operation of a propionate-degrading fluidized-bed reactor. *Appl Microbiol Biotechnol* **36**, 810-816.

Hori, T., Haruta, S., Ueno, Y., Ishii, M., and Igarashi, Y. (2006) Dynamic transition of a methanogenic population in response to the concentration of volatile fatty acids in a thermophilic anaerobic digester. *Appl Environ Microbiol* **72**, 1623-1630.

Kuhner, C.H., Frank, C., Griesshammer, A., Schmittroth, M., Acker, G., Gossner, A. and Drake, H.L. (1997) *Sporomusa silvacetica* sp, nov., an acetogenic bacterium isolated from aggregated forest soil. *Int J Syst Bacteriol* **47**, 352-358.

Laanbroek, H., Abee, T. and Voogd, J. (1982) Alcohol conversion by *Desulfolobus propionicus* Lindhorst in the presence and absence of sulfate and hydrogen. *Arch Microbiol* **133**, 178-184.

Lettinga, G., Hobma, S.W., Hulshoff Pol, L.W., de Zeeuw, W., de Jong, P., Grin, P.C. and Roersma, R.E. (1983) Design operation and economy of anaerobic treatment. *Water Sci Technol* **15**(8-9), 177-195.

Loisel, P., Harmand, J., Zemb, O., Latrille, E, Lobry, C., Delgenès, J.P. and Godon, J.J. (2006) Denaturing gradient electrophoresis (DGE) and single-strand conformation polymorphism (SSCP) molecular fingerprintings revisited by simulation and used as a tool to measure microbial diversity. *Environ Microbiol.* **8**, 720-731.

Lonergan, D.J., Jenter, H.L., Coates, J.D., Schmidt, T.M. and Lovley, D.R. (1996) Phylogenetic analysis of dissimilatory Fe(III)-reducing bacteria. *J Bacteriol* **178**, 2402-2408.

Lovley, D.R., Phillips, E.J.P. , Lonergan, D.J. and Widman, P.K. (1995). Fe(III) and S^0 reduction by *Pelobacter Carbinolicus*. *Appl Environ Microbiol* **61**, 2132-2138.

Michaud, S., Bernet, N., Buffière, P. and Delgenès, J.P. (2005) Use of the methane yield to indicate the metabolic behaviour of methanogenic biofilms. *Process Biochem* **40**, 2751-2755.

Nicolella, C., van Loosdrecht, M.C.M. and Heijnen, J.J. (2000). Wastewater treatment with particulate biofilm reactors. *J Biotechnol* **80**, 1–33.

Percheron, G., Bernet, N. and Moletta, R. (1997) Start-up of anaerobic digestion of sulfate wastewater. *Biores Technol* **61**, 21 - 27.

Punal, A., Melloni, P., Roca, E., Rozzi, A. and Lema, J.M. (2001) Automatic start-up of UASB reactors. *J Environ Eng ASCE* **127**, 397-402.

Raskin, L., Rittmann, B.E. and Stahl, D.A. (1996) Competition and coexistence of sulfate-reducing and methanogenic populations in anaerobic biofilms. *Appl Environ Microbiol* **62**, 3847-3857.

Schink, B., Kremer, D. and Hansen, T. (1987) Pathway of propionate formation from ethanol in *Pelobacter propionicus*. *Arch Microbiol* **147**, 321-327.

Schmidt, J.E. and Ahring, B.K. (1999) Immobilization patterns and dynamics of acetate-utilizing methanogens immobilized in sterile granular sludge in upflow anaerobic sludge blanket reactors. *Appl Environ Microbiol* **65**(3), 1050-1054.

Steyer, J.P., Buffière, P., Rolland, D. and Moletta, R. (1999) Advanced control of anaerobic digestion processes through disturbances monitoring. *Water Res.* **33**, 2059-2068.

Stronach, S.M., Rudd, T. and Lester, J.N. (1986) The influence of variable organic loading on the start-up of an anaerobic fluidised bed reactor. *Biotechnol. Lett.* **8**, 521-524.

Tholozan, J.L., Samain, E., Grivet, J.P. and Albagnac, G. (1990) Propionate metabolism in a methanogenic enrichment culture. Direct reductive carboxylation and acetogenesis pathways. *FEMS Microbiol Lett* **73**, 291-297.

Tijhuis, L., van Loosdrecht, M.C.M. and Heijnen, J.J. (1994) Formation and growth of heterotrophic aerobic biofilms on small suspended particles in airlift reactors. *Biotechnol Bioeng* **44**, 595-608.

Weiland, P. and Rozzi, A. (1991) Start-up, operation, monitoring and control of high-rate anaerobic treatment systems - Discusser's report - Anaerobic treatment technology for municipal and wastewater. *Water Sci Technol* **24**(8), 257-277.

Widdel, F. (1988) Microbiology and ecology of sulfate - and sulfur-reducing bacteria. In *Biology Anaerobic Microorganisms*. ed. A.J.B. Zehnder. pp. 469-585. New York, John Wiley & Sons.

Wu, M. and Hickey, R. (1996). n-Propanol production during ethanol degradation using anaerobic granules. *Water Res* **30**, 1686-1694.

Wu, W.M., Hickey, R.F. and Zeikus, J.G. (1991) Characterization of metabolic performance of methanogenic granules treating brewery wastewater, role of sulfate-reducing bacteria. *Appl Environ Microbiol* **57**, 3438-3449.

Zumstein, E., Moletta, R. and Godon, J.J. (2000) Examination of two years of community dynamics in an anaerobic bioreactor using fluorescence polymerase chain reaction (PCR) single-strand conformation polymorphism analysis. *Environ Microbiol* **2**(1), 69-78.

LEGENDS

Figure 1 Variation of OLR, COD removal efficiency and Ethanol to VFA conversion (as percentage of the carbon input) during the 81 days of both reactors start up.

Figure 2 Alignment of the bacterial community SSCP patterns obtained by PCR amplification of the 16S rDNA V3 regions of the inoculum (top of the figure) and carrier particle biofilms on days 1 (middle) and 23 (bottom) for reactors A (on the left) and B (on the right).

Figure 3 **Schematic representation of the** biofilm bacterial diversity dynamics within reactors A and B. Each profile was scanned and represented as a row of discs where each disc corresponds to a distinguishable peak. Disc areas are proportional to the proportion of their corresponding peaks in the total profile.

Figure 4 Alignment of the archaeal community SSCP patterns obtained by PCR amplification of the 16S rDNA V3 regions of the inoculum and carrier particle biofilms from days 1 to 72 for reactors A (left) and B (right).

Figure 5 FISH of colonized carrier particles (R_B, day 70) observed by confocal laser scanning microscopy – Double hybridization with probes *Archaea* ARC915 – FAM (red) and *Bacteria* EUB338 - CY3 (green), with low (A) and high magnification (B).

Figure 6 Proposition for a schematic representation of main anaerobic pathways of ethanol degradation to methane and carbon dioxide (basic lines and bold type) and groups of microorganisms involved for both reactors. Dashed lines symbolize the sulphate reducing metabolic pathway and illustrate competition with methanogenic and acidogenic microorganisms.

Table 1 Carbon mass balance in percentage of carbon input as ethanol. Data are the mean of measurements realized during the considered period.

Reactor A:

Phase	Length (d)	VFA	Bicarbonate	CH_4	CO_2	AVS	VSS	Total
I	10	8.0%	35.6%	19.1%	3.8%	19.5%	4.5%	90.5%
II	28	23.2%	23.8%	37.5%	1.5%	5.4%	2.6%	94.1%
III	21	41.3%	13.7%	32.2%	1.1%	2.4%	3.4%	94.1%
IV	22	6.1%	17.4%	54.3%	9.3%	4.0%	2.9%	94.0%
Overall	**81**	**18.6%**	**17.6%**	**45.1%**	**5.7%**	**3.9%**	**3.1%**	**94.1%**

Reactor B:

Phase	Length (d)	VFA	Bicarbonate	CH_4	CO_2	AVS	VSS	Total
I	10	6.3%	44.2%	17.6%	4.6%	19.7%	3.9%	96.3%
II	28	11.0%	29.3%	41.1%	2.4%	6.1%	3.2%	93.2%
III	21	27.1%	22.2%	36.9%	2.7%	1.9%	3.5%	94.2%
IV	22	3.1%	22.1%	53.0%	9.4%	5.4%	2.8%	95.7%
Overall	**81**	**11%**	**23.3%**	**47%**	**6.4%**	**4.6%**	**3.1%**	**95.5%**

Table 2 Phylogenetic affiliation of 16S rDNA sequences

Peak name	Phylum	% ID	Closest microorganism or environmental clone	Accession No	Isolated from
A	*Clostridia*	100	Uncultured bacterium clone SmB60f1	AB266923	Anaerobic UASB reactor
B	*Bacteria* (environmental samples)	98	Uncultured bacterium clone MKEW-104	AJ852366	Gut Compartments of Melolontha melolontha Larvae (Coleoptera: Scarabaeidae)
C	*Bacteria Chloroflexi*	99	Clone SJA - 117	AJ009488	Anaerobic trichlorobenzene-transforming microbial consortium
D	*Deltaproteobacteria Desulfovibrio*	98	*Desulfovibrio* sp. A2	AY770382	zinc-smelter wastewater effluents
E	*Deltaproteobacteria Desulfovibrio*	98	*Desulfovibrio* sp. A2	AY770382	zinc-smelter wastewater effluents
F	*Deltaproteobacteria Pelobacter*	99	*Pelobacter* sp. clone M113	AY692043	anaerobic biofilm UASB reactor
G	*Deltaproteobacteria Geobacteraceae*	100	Anaerobic syntrophic bacterium NE23-3	AB231802	anaerobic ethanol-oxidizing bacterium from an anaerobic digested sludge
H	*Deltaproteobacteria Geobacteraceae*	99	Uncultured bacterium clone SJA-152	AJ009496	anaerobic, trichlorobenzene-transforming microbial consortium
I	*Bacteria* (environmental samples)	97	Uncultured eubacterium AA01	AF275913	anaerobic digester fed with glucose
J	*Firmicutes Sporomusa*	94	*Sporomusa* sp. DR6	Y17760	anoxic bulk soil of flooded rice microcosms
K	*Firmicutes Sporomusa*	95	*Sporomusa ovata*	AJ279800	spore-forming anaerobe that ferments sugar alcohols
N	*Archaea*	99	Uncultured archaeon clone CG-8	AB233298	methanogenic UASB granular sludge
O	*Euryarchaeota Methanobacterium*	99	*Methanobacterium beijingense*	AY552778	anaerobic digesters

FIG 1

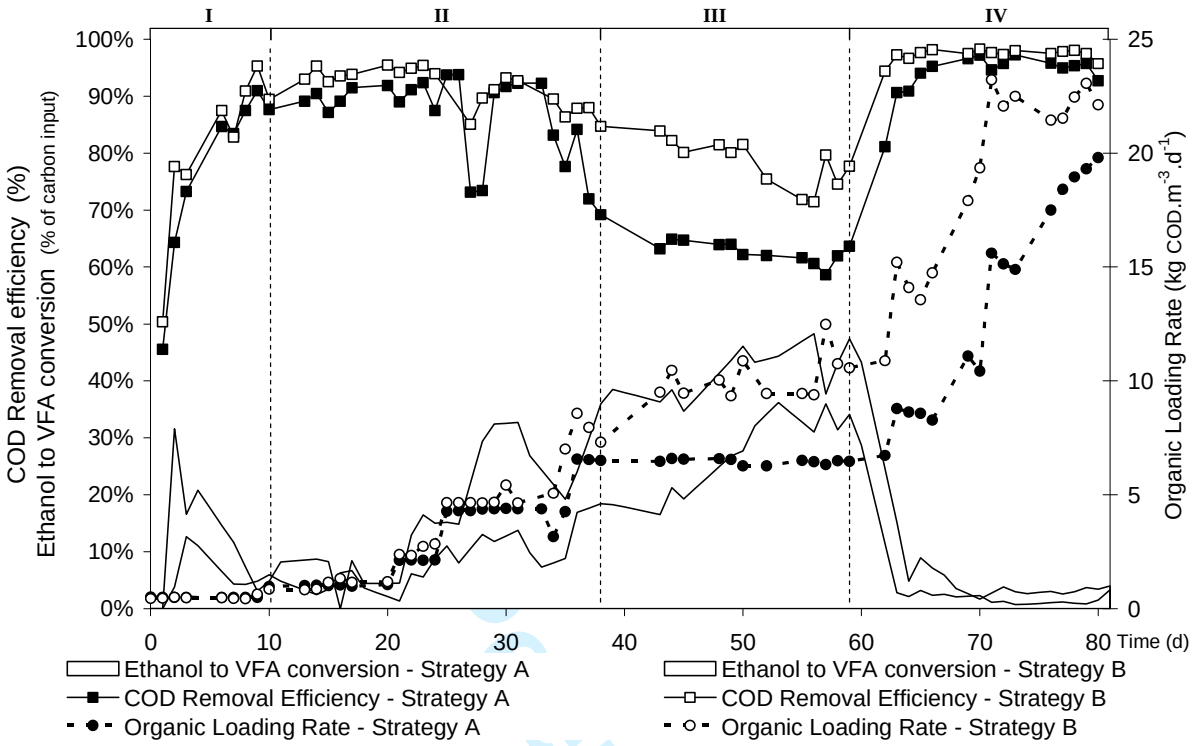

FIG 2

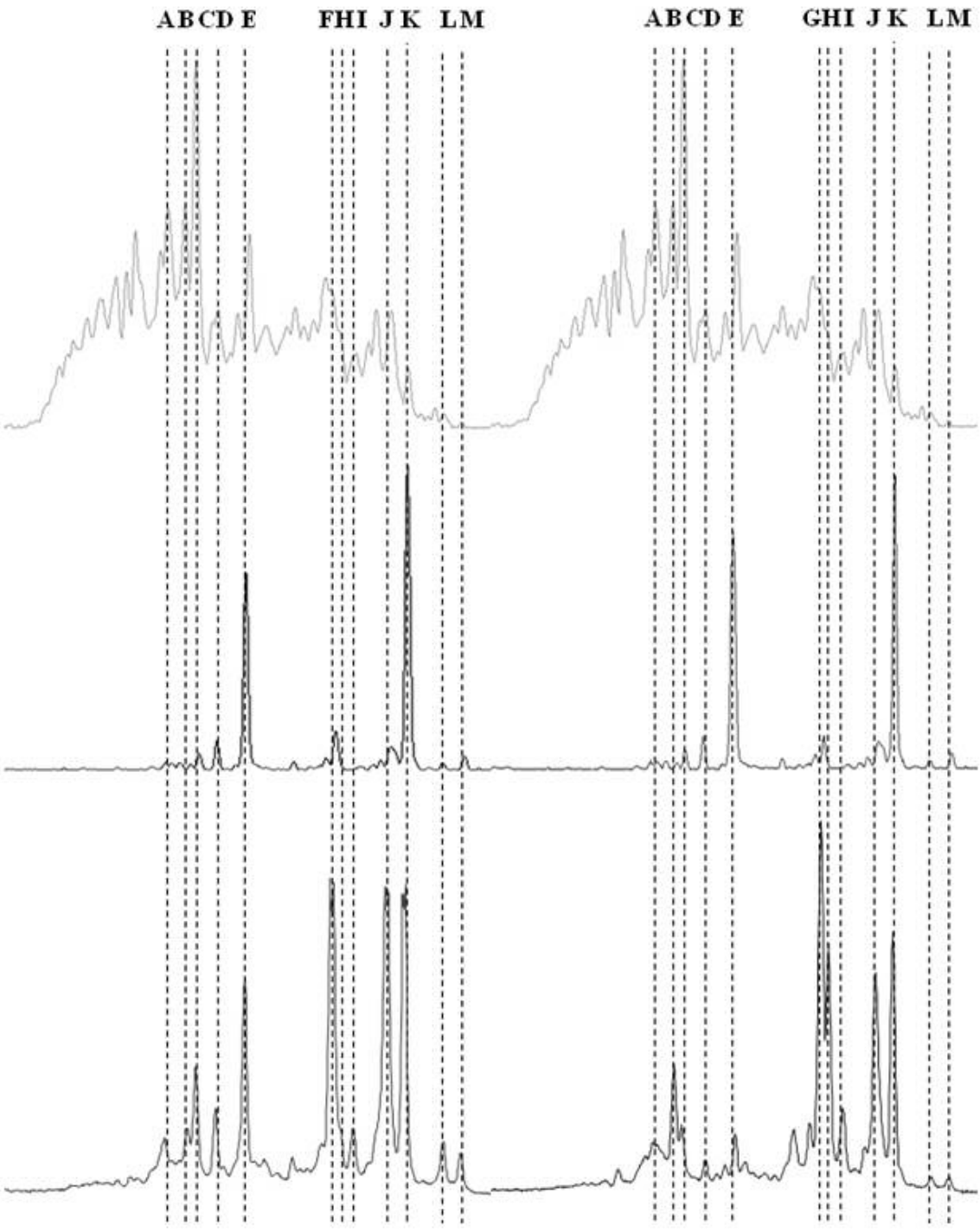

FIG 3

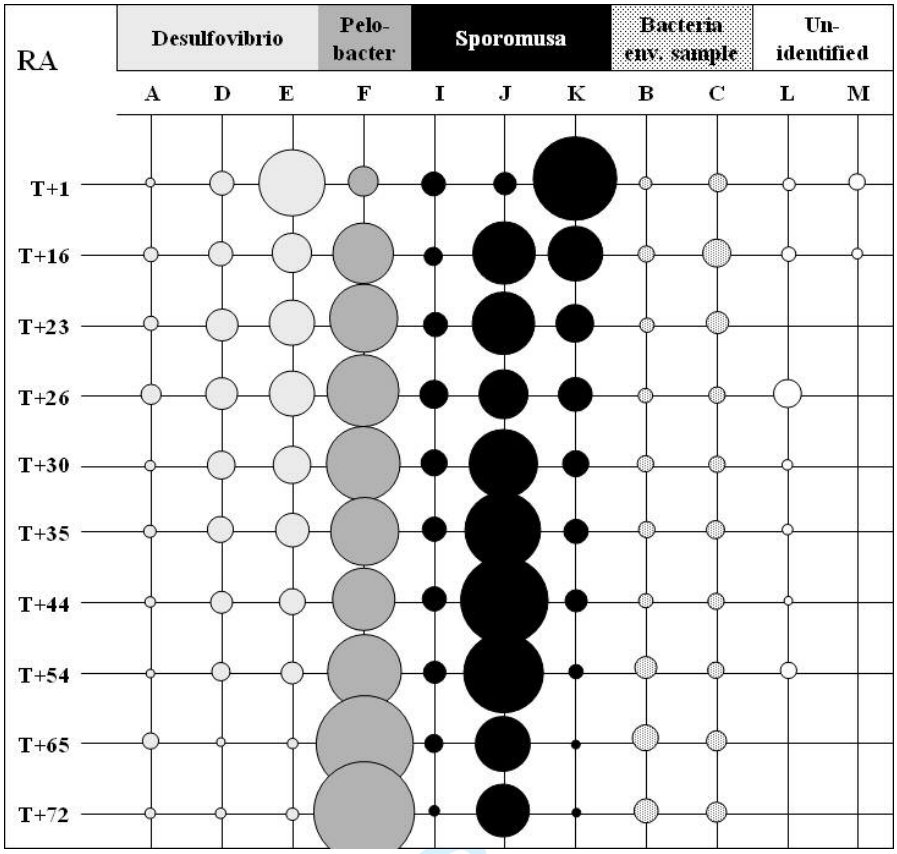
RA
Desulfovibrio
Pelo-bacter
Sporomusa
Bacteria env. sample
Un-identified
A D E F I J K B C L M
T+1
T+16
T+23
T+26
T+30
T+35
T+44
T+54
T+65
T+72

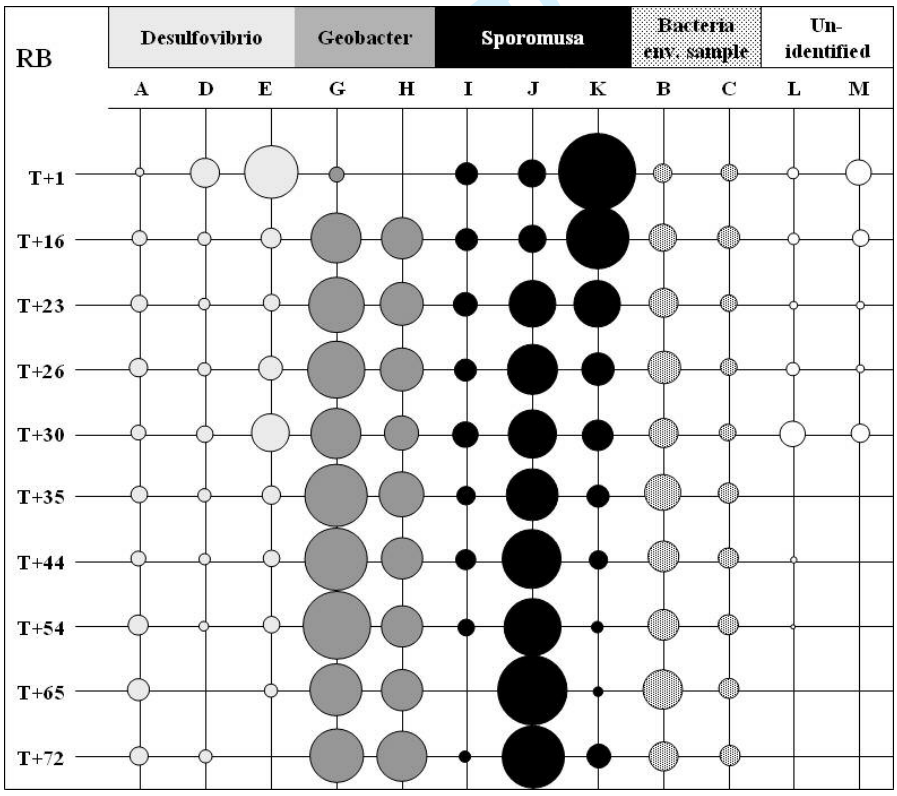
RB
Desulfovibrio
Geobacter
Sporomusa
Bacteria env. sample
Un-identified
A D E G H I J K B C L M
T+1
T+16
T+23
T+26
T+30
T+35
T+44
T+54
T+65
T+72

FIG 4

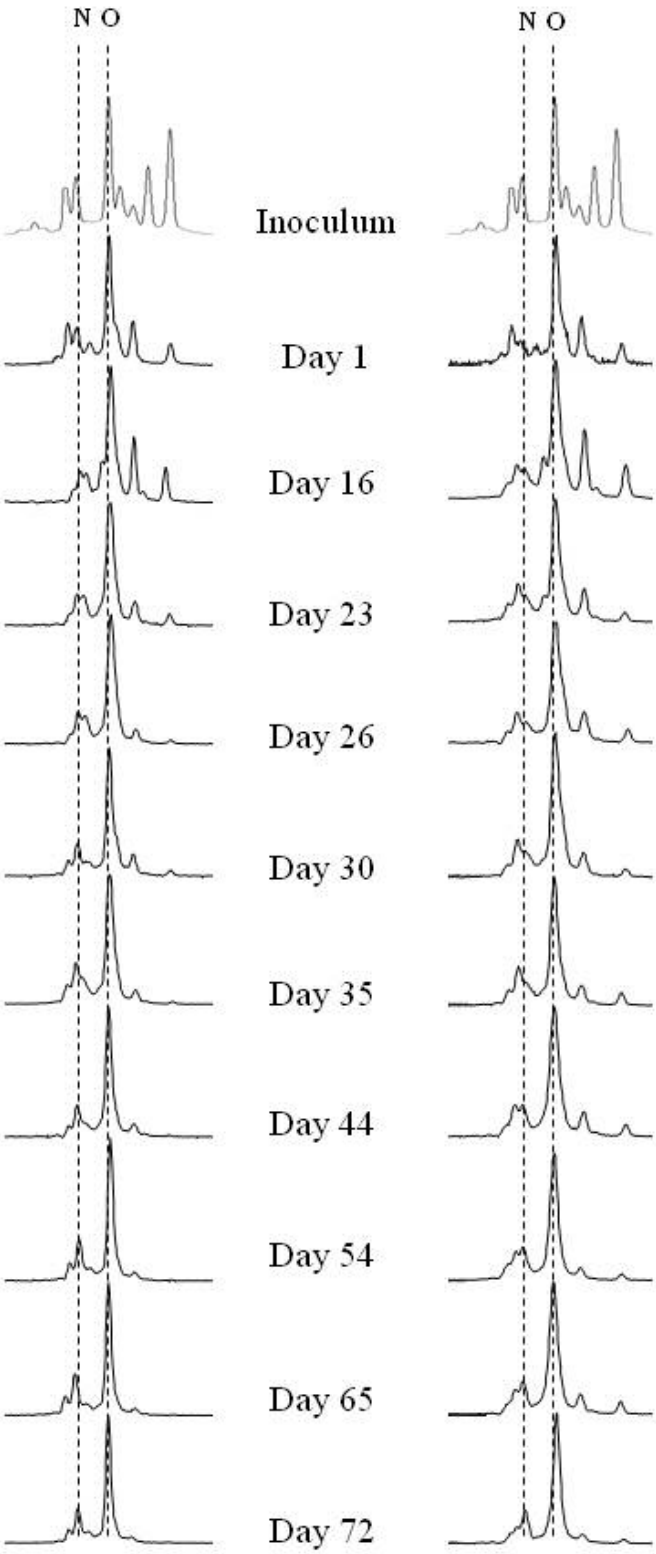
N O
N O
Inoculum
Day 1
Day 16
Day 23
Day 26
Day 30
Day 35
Day 44
Day 54
Day 65
Day 72

FIG 5

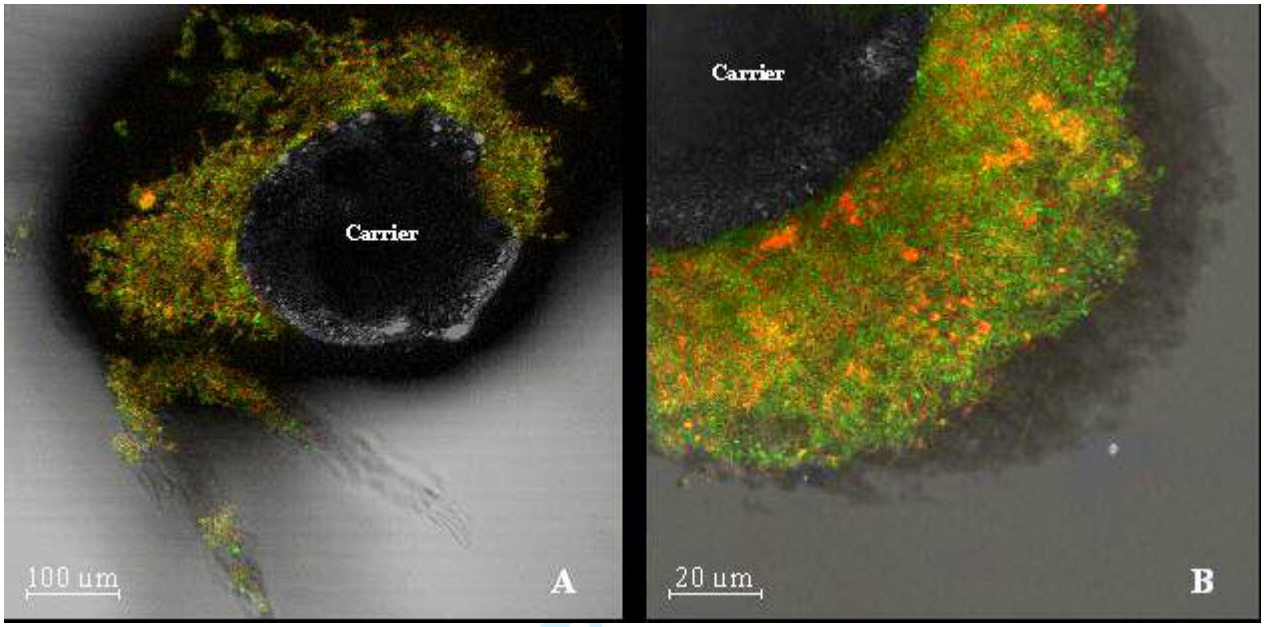

FIG 6

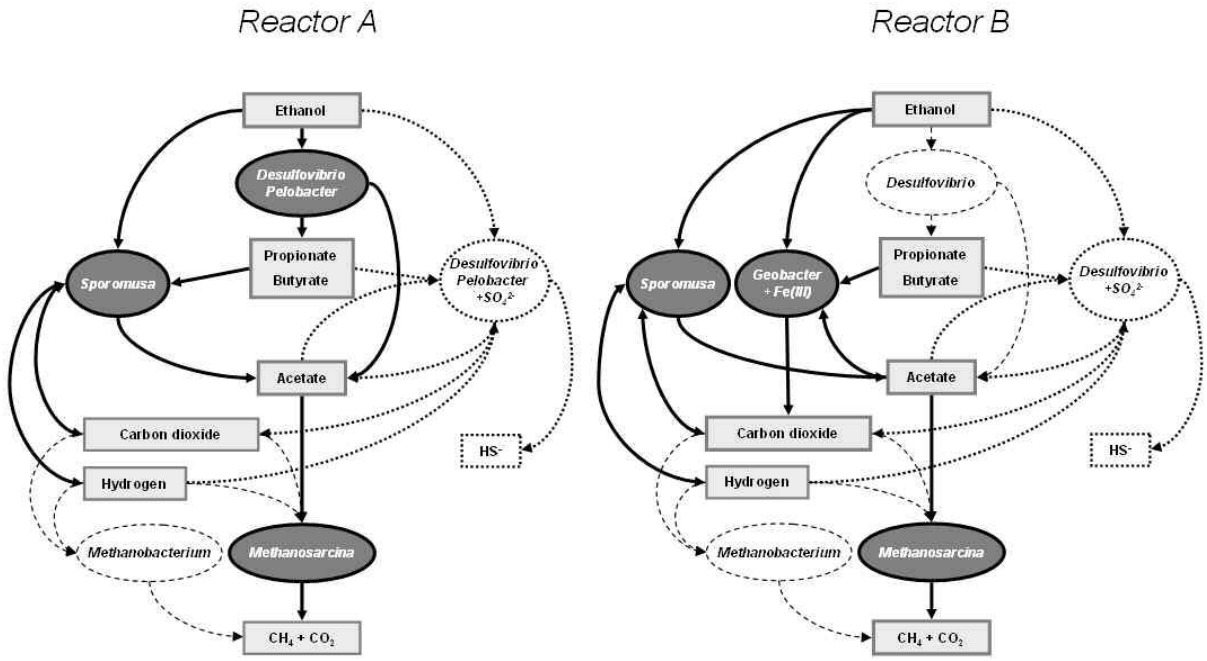
Reactor A
Ethanol
Desulfovibrio Pelobacter
Propionate Butyrate
Sporomusa
Desulfovibrio Pelobacter +SO4 2-
Acetate
Carbon dioxide
HS-
Hydrogen
Methanobacterium
Methanosarcina
CH4 + CO2
Reactor B
Ethanol
Desulfovibrio
Propionate Butyrate
Sporomusa
Geobacter +Fe(III)
Desulfovibrio +SO4 2-
Acetate
Carbon dioxide
HS-
Hydrogen
Methanobacterium
Methanosarcina
CH4 + CO2